Article ID: 1007-4627(2024) 01-0001-07

Effects of rotation, blocking and octupole deformation on pairing correlations in the U and Pu isotopes

ZHANG Jun[1], HE Xiao-tao[2]

(*1. College of Physics, Nanjing University of Aeronautics and Astronautics, Nanjing 210016, China;*
2. College of Materials Science and Technology, Nanjing University of Aeronautics and Astronautics, Nanjing 210016, China)

Abstract: By including octupole correlations in the Nilsson potential, the ground-state rotational bands in the reflection-asymmetric (RA) nuclei are investigated by using the cranked shell model (CSM) with the monopole and quadrupole pairing correlations treated by a particle-number-conserving (PNC) method. The experimental kinematic moments of inertia (MoIs) of alternating-parity bands in the even-even nuclei ^{236,238}U and ^{238,240}Pu, and parity-doublet bands in the odd-A nuclei ^{237}U and ^{239}Pu are well reproduced by the PNC-CSM calculations. Compared to the neighboring even-even nuclei ^{236,238}U and ^{238,240}Pu, 50% $\sim$ 60% increase of $\boldsymbol{J}^{(1)}$ can be seen for the intrinsic $s = -i$ bands in ^{237}U and ^{239}Pu. Those mainly attribute to the pairing reduction due to the Pauli blocking of the unpaired neutron occupying the neutron orbitals near the Fermi surface. The gradual increase of $\boldsymbol{J}^{(1)}$ versus rotational frequency can be explained by the pairing reduction due to the rotation. The present calculation shows that the MoIs of the reflection-asymmetric nuclei are higher than those of the reflection-symmetric (RS) nuclei at the low rotational frequency. Furthermore, compared with the RS nuclei, the pairing reduction of the RA nuclei increase when a larger octupole deformation ε_3 is included in the calculation.

Key words: octupole correlations; cranked shell model; particle-number-conserving method; alternating-parity bands; parity-doublet bands; pairing correlations

CLC number: O571.53 **Document code:** A **DOI:** 10.11804/NuclPhysRev.31.01.01

1 Introduction

The typical features for octupole correlations in the ground-state reflection-asymmetric nuclei are the occurrence of alternating-parity bands in the even-mass nuclei and parity-doublet bands in the odd-mass nuclei[1]. These correlations in nuclei are caused by the long-range octupole-octupole interaction between single-particle states with $\Delta l = \Delta j = 3$. In the light actinide mass region, the proton Fermi surface lies between $f_{7/2}$ and $i_{13/2}$ orbitals, and the neutron Fermi surface lies between $g_{9/2}$ and $j_{15/2}$ orbitals in nuclei with $Z \approx 88$ and $N \approx 134$. Since the proximity of these levels, strong octupole coupling lead to intrinsic reflection asymmetric shapes in the ground-state nuclei.

In the actinide mass region, most odd-mass and even-even nuclei behave striking features of octupole correlations in the experiment[2-6]. It is found experimentally that the rotational behaviors of the yrast and negative-parity bands in ^{236,237,238}U and those in ^{238,239,240}Pu are striking different, which are linked to variations with mass of the strength of octupole correlations[7-11]. In term of theoretical investigations, many approaches have been developed to describe the octupole correlations in the reflection-asymmetric nuclei. These include reflection-asymmetric mean-field approach[12], cluster models[13], vibrational approaches[14], reflection asymmetric shell model[15] and cranked shell model[16].

In the present work, the cranked shell model with the pairing correlations treated by a particle-number-conserving method is developed to investigated the alternating-parity bands in even-even nuclei ^{236,238}U and ^{238,240}Pu, and the parity-doublet bands in odd-A nuclei ^{237}U and ^{239}Pu. In the

Received date: 18 Mar. 2024; **Revised date:** 18 Mar. 2024
Foundation item: Natural Science Foundation of China (U2032138, 11775112);
Biography: ZHANG Jun(1990–), Hefei, Anhui Province, phd student, Working on nuclear structure; E-mail: zhangjun3069@nuaa.edu.cn
Corresponding author: E-mail: hext@nuaa.edu.cn

particle-number-conserving method, the cranked shell model Hamiltonian is diagonalized directly in the truncated Fock space. Thus, the particle number is conserved exactly and the Pauli blocking effect is taken into account spontaneously. The effects of rotation, Pauli blocking effects and the octupole deformation on the pairing correlations in the U and Pu isotopes have been investigated by the PNC-CSM method in detail.

2 Theoretical framework

In the framework of the cranked shell model, the Hamiltonian of an axially deformed nucleus in the rotating frame [17-20] is

$$H_{\rm CSM} = H_{\rm Nil} - \omega J_x + H_{\rm P}(0) + H_{\rm P}(2), \tag{1}$$

where $H_{\rm Nil} = \sum h_{\rm Nil}(\varepsilon_2, \varepsilon_3, \varepsilon_4)$ is the Nilsson Hamiltonian, in which the quadrupole (ε_2), octupole (ε_3) and hexadecapole (ε_4) deformation parameters are included [16,21]. $-\omega J_x$ is the Coriolis interaction with the rotational frequency ω about the x axis (perpendicular to the symmetry z axis here).

When $\omega = 0$, the single-particle Hamiltonian $h_{\rm Nil}$ has nonzero matrix elements of Y_{30} between different shell N. Since $p = (-1)^N$, the parity is no longer a good quantum number, but Ω (the single-particle angular momentum projection on the symmetry axis) is still a good quantum number. However, when $\omega \neq 0$, the symmetry with respect to the reflection through plane yoz, S_x operator, still holds. The single-particle orbitals can be labeled with the simplex quantum number s (the eigenvalues of S_x operator, $s = \pm i$).

The pairing includes the monopole and quadrupole pairing correlations,

$$H_{\rm P}(0) = -G_0 \sum_{\xi\eta} a^\dagger_\xi a^\dagger_{\bar\xi} a_{\bar\eta} a_\eta, \tag{2}$$

$$H_{\rm P}(2) = -G_2 \sum_{\xi\eta} q_2(\xi) q_2(\eta) a^\dagger_\xi a^\dagger_{\bar\xi} a_{\bar\eta} a_\eta, \tag{3}$$

where $\xi(\eta)$ is the eigenstate of the Nilsson Hamiltonian $h_{\rm Nil}$, and $\bar\xi(\bar\eta)$ is the time-reversed state, $q_2(\xi) = \sqrt{16\pi/5}\langle\xi|r^2 Y_{20}|\xi\rangle$ is the diagonal element of the stretched quadrupole operator, and G_0 and G_2 are the effective strengths of monopole and quadrupole pairing interactions, respectively.

By diagonalizing the cranked shell model Hamiltonian in a sufficiently large cranked many-particle configuration (CMPC), a sufficiently accurate low-lying excited intrinsic wave function of the reflection-asymmetric nuclei are obtained as

$$|\psi\rangle = \sum_i C_i |i\rangle, \tag{4}$$

where $|i\rangle = |\mu_1\mu_2\cdots\mu_n\rangle$ is a CMPC for an n-particle system, and $\mu_1\mu_2\cdots\mu_n$ are the occupied cranked Nilsson orbitals. Each configuration $|i\rangle$ is characterized by the simplex s_i,

$$s_i = s_{\mu_1} s_{\mu_2} \cdots s_{\mu_n}, \tag{5}$$

where s_μ is the simplex of the particle occupying in orbital μ. The kinematic moment of inertia of eigenstate $|\psi\rangle$ can be written as

$$J^{(1)} = \frac{\langle\psi|J_x|\psi\rangle}{\omega} \tag{6}$$

Experimentally, the rotational band with simplex quantum number s is characterized by spin states I of alternating parity [22]

$$p = s e^{-i\pi I}. \tag{7}$$

Therefore for reflection-asymmetric systems with even number of nucleons we have

$$s = +1, \quad I^p = 0^+, 1^-, 2^+, 3^-, \cdots, \tag{8}$$

$$s = -1, \quad I^p = 0^-, 1^+, 2^-, 3^+, \cdots, \tag{9}$$

while for systems with odd number of nucleons we have

$$s = +i, \quad I^p = 1/2^+, 3/2^-, 5/2^+, 7/2^-, \cdots, \tag{10}$$

$$s = -i, \quad I^p = 1/2^-, 3/2^+, 5/2^-, 7/2^+, \cdots. \tag{11}$$

The moments of inertia for alternating parity bands can be expressed as

$$J^{(1)}_p = \frac{\langle\psi|J_x|\psi\rangle}{\omega} - \frac{1}{2} p \Delta J^{(1)}(\omega) \tag{12}$$

where $|\psi\rangle$ is the parity-independent wave function with the rotational frequency ω obtained by the PNC-CSM method. The $\Delta J^{(1)}(\omega)$ are parity splitting of the moments of inertia in the experimental alternating-parity bands, which can be obtained by

$$\Delta J^{(1)}(\omega) = J^{(1)}_-(\omega) - J^{(1)}_+(\omega) \tag{13}$$

in which $J^{(1)}_-(\omega)$ and $J^{(1)}_+(\omega)$ are the experimental MoIs of the negative- and positive-parity rotational bands corresponding to the rotational frequency ω.

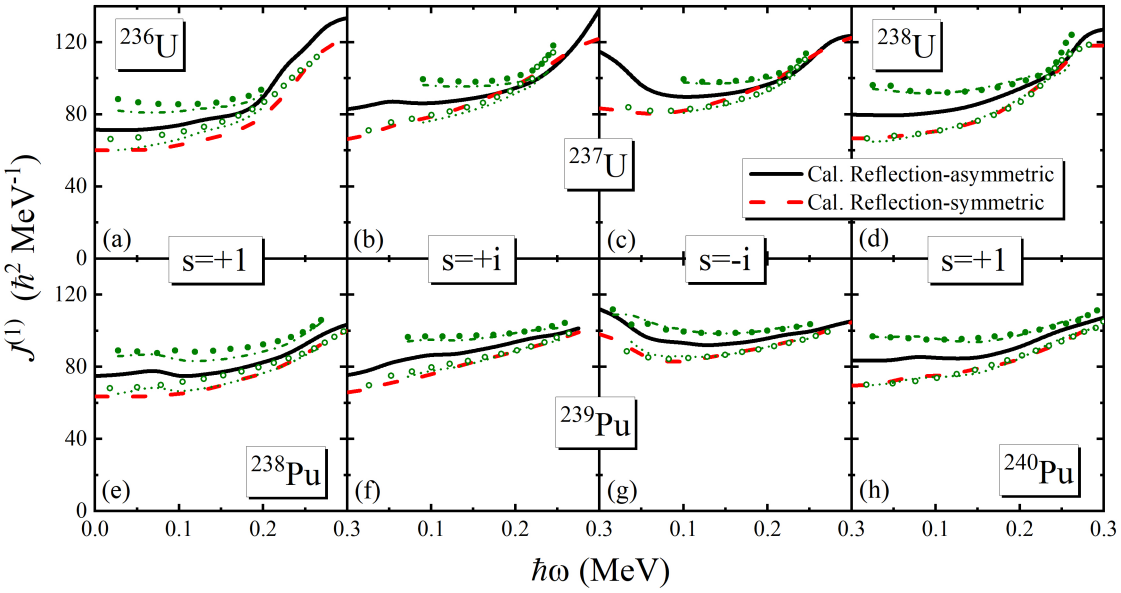

Fig. 1　(Color online) The experimental and calculated kinematic moments of inertia $\boldsymbol{J}^{(1)}$ for the alternating-parity bands in even-even nuclei ^{236,238}U and ^{238,240}Pu, and parity-double bands in odd-A nuclei ^{237}U and ^{239}Pu. The experimental data for the negative (positive) parity band are denoted by solid (open) circle. The PNC-CSM calculations in the reflection-asymmetric nuclei are denoted by black solid lines. After considering the parity spitting of Eqs. (12) and (13), the negative and positive parity bands are denoted by dash-dotted and dotted lines, respectively. The PNC-CSM calculations in the reflection-symmetric nuclei (without ε_3 deformation) are shown by red dashed lines.

3　Results and Discussions

3.1　Parameters

In this work, the Nilsson parameters (κ, μ) are taken from Ref.[23]. The deformations ε_2, ε_3, and ε_4 are input parameters in the PNC-CSM method. The values of ε_2 and ε_4 are chosen close to the calculated deformations of the ground state in the actinide region[24]. The ε_3 values used in this work are chosen by fitting the experimental MoIs and alignments of the ground-state bands in the U and Pu isotopes. The deformation parameters (ε_2, ε_3, ε_4) used in our PNC-CSM calculations are (0.200, 0.110, -0.055), (0.220, 0.130, -0.040), (0.228, 0.025, -0.065) and (0.230, 0.010, -0.045) for even-even nuclei ^{236}U, ^{238}U, ^{238}Pu and ^{240}Pu, respectively. The deformations of odd-A nuclei ^{237}U and ^{239}Pu are taken as the average of the neighboring even-even nuclei.

The effective pairing strengths G_0 and G_2, in principle, can be determined by the odd-even differences in nuclear binding energies. The values are connected with the dimensions of the truncated cranked many-particle configuration space. For even-even nuclei ^{236,238}U and ^{238,240}Pu, the effective monopole and quadrupole pairing strengths are $G_{0p} = 0.25$ MeV, $G_{2p} = 0.03$ MeV and $G_{0n} = 0.25$ MeV, $G_{2n} = 0.015$ MeV for protons and neutrons, respectively. For odd-A nuclei ^{237}U and ^{239}Pu, the neutron pairing strengths are little smaller than those in even-even nuclei. For all nuclei studied in this work, the CMPC space is constructed in the proton $N = 5, 6$ and neutron $N = 6, 7$ shells. The dimensions of the CMPC space are about 1000 for both protons and neutrons.

3.2　Moments of inertia

Figure 1 shows the experimental and calculated kinematic moments of inertia $\boldsymbol{J}^{(1)}$ for the alternating-parity bands ($s = +1$) in even-even nuclei ^{236,238}U and ^{238,240}Pu, and parity-doublet bands ($s = \pm i$) in odd-A nuclei ^{237}U and ^{239}Pu. The experimental data for the negative (positive) parity band are denoted by green solid (open) circle. The PNC-CSM calculations in the reflection-asymmetric nuclei are denoted by black solid lines. After considering the parity spitting of Eqs. (12) and (13), the negative and positive parity bands are denoted by dash-dotted and dotted lines, respectively. The PNC-CSM calculations in the reflection-symmetric nuclei (without ε_3 deformation) are shown by red dashed lines. It can be seen that the experimental moments of inertia versus the rotational frequency $\hbar\omega$ are produced very

well by the PNC-CSM calculations. As shown in Figs. 1(b), 1(c), 1(f), and 1(g), there are simplex splitting (solid black line) between $s = +i$ and $s = -i$ partner bands at $\hbar\omega$ <0.10 MeV in both odd-A nuclei ^{237}U and ^{239}Pu.

From Fig. 1, we can see that the moments of inertia $\boldsymbol{J}^{(1)}$ gradually increase versus rotational frequency in all nuclei. To see the increase of $\boldsymbol{J}^{(1)}$ in these nuclei more clearly, we show the differences in MoIs of intrinsic rotational bands in ^{236}U at different rotational frequency. For other nuclei, the results are very similar, and will not shown here. The calculated results for ^{236}U are:

$$\frac{\delta J}{J} = \frac{J(^{236}\mathrm{U}, \hbar\omega = 0.30\mathrm{MeV}) - J(^{236}\mathrm{U}, \hbar\omega = 0)}{J(^{236}\mathrm{U}, \hbar\omega = 0)} \approx 87.3\%.$$

It can be seen that there are significant increase of $\boldsymbol{J}^{(1)}$ with the rotational frequency increasing.

In order to investigate the Pauli blocking effects on the odd-even differences in the MoIs $\delta J/J$, we study the MoIs of the intrinsic $s = -i$ rotational bands in odd-A nuclei ^{237}U and ^{239}Pu and those in the neighboring even-even nuclei ^{236}U and ^{238}Pu at the bandhead $\hbar\omega = 0.00$ MeV.

$$\frac{\delta J}{J} = \frac{J(^{237}\mathrm{U}, \mathrm{RA}) - J(^{236}\mathrm{U}, \mathrm{RA})}{J(^{236}\mathrm{U}, \mathrm{RA})} \approx 61.0\%,$$
$$\frac{\delta J}{J} = \frac{J(^{239}\mathrm{Pu}, \mathrm{RA}) - J(^{238}\mathrm{Pu}, \mathrm{RA})}{J(^{238}\mathrm{Pu}, \mathrm{RA})} \approx 49.6\%.$$

Therefore, the significant increase of moments of inertia $\boldsymbol{J}^{(1)}$ in the odd-A nuclei mainly attribute to the Pauli blocking effects of the unpaired neutron, compared with the neighboring even-even nuclei.

Furthermore, as shown in Fig. 1, the calculated MoIs of the intrinsic rotational bands in the reflection-asymmetric nuclei are obviously higher than those in reflection-symmetric nuclei. To show the effect of octupole deformation ε_3 on the MoIs, we study the differences in MoIs $\delta J/J$ between the reflection-asymmetric and reflection-symmetric rotational bands at the bandhead $\hbar\omega = 0.00$ MeV. The calculated results for the U isotopes are:

$$\frac{\delta J}{J} = \frac{J(^{236}\mathrm{U}, \mathrm{RA}) - J(^{236}\mathrm{U}, \mathrm{RS})}{J(^{236}\mathrm{U}, \mathrm{RS})} \approx 18.7\%,\ s = +1,$$
$$\frac{\delta J}{J} = \frac{J(^{237}\mathrm{U}, \mathrm{RA}) - J(^{237}\mathrm{U}, \mathrm{RS})}{J(^{237}\mathrm{U}, \mathrm{RS})} \approx 24.7\%,\ s = +i,$$
$$\frac{\delta J}{J} = \frac{J(^{237}\mathrm{U}, \mathrm{RA}) - J(^{237}\mathrm{U}, \mathrm{RS})}{J(^{237}\mathrm{U}, \mathrm{RS})} \approx 37.8\%,\ s = -i,$$
$$\frac{\delta J}{J} = \frac{J(^{238}\mathrm{U}, \mathrm{RA}) - J(^{238}\mathrm{U}, \mathrm{RS})}{J(^{238}\mathrm{U}, \mathrm{RS})} \approx 19.7\%,\ s = +1,$$

and the calculated results for the Pu isotopes are:

$$\frac{\delta J}{J} = \frac{J(^{238}\mathrm{Pu}, \mathrm{RA}) - J(^{238}\mathrm{Pu}, \mathrm{RS})}{J(^{238}\mathrm{Pu}, \mathrm{RS})} \approx 17.7\%,\ s = +1,$$
$$\frac{\delta J}{J} = \frac{J(^{239}\mathrm{Pu}, \mathrm{RA}) - J(^{239}\mathrm{Pu}, \mathrm{RS})}{J(^{239}\mathrm{Pu}, \mathrm{RS})} \approx 14.3\%,\ s = +i,$$
$$\frac{\delta J}{J} = \frac{J(^{239}\mathrm{Pu}, \mathrm{RA}) - J(^{239}\mathrm{Pu}, \mathrm{RS})}{J(^{239}\mathrm{Pu}, \mathrm{RS})} \approx 14.1\%,\ s = -i,$$
$$\frac{\delta J}{J} = \frac{J(^{240}\mathrm{Pu}, \mathrm{RA}) - J(^{240}\mathrm{Pu}, \mathrm{RS})}{J(^{240}\mathrm{Pu}, \mathrm{RS})} \approx 20.0\%,\ s = +1.$$

We can see that the differences in the U isotopes are almost larger that those in the Pu isotopes. In this work, the ε_3 deformations of U isotopes are about 0.10, while those in the Pu isotopes are about 0.02. Thus, it can been seen clearly that ε_3 deformation give a very important contribution to the increase of the moments of inertia $\boldsymbol{J}^{(1)}$.

In general, the increase of $\boldsymbol{J}^{(1)}$ at low frequency, and the gradual increase of versus rotational frequency can be mainly attributed to the pairing reduction. In order to have a more clear understanding of the increase of $\boldsymbol{J}^{(1)}$, we study the effects of rotation, Pauli blocking effects and the octupole deformation on the pairing correlations in the U and Pu isotopes in detail.

3.3 Pairing correlations

In the PNC-CSM formalism, the nuclear pairing gap is defined as[25]

$$\tilde{\Delta} = G_0 \left[-\frac{1}{G_0} \langle \psi | H_{\mathrm{P}} | \psi \rangle \right]^{1/2} \tag{14}$$

Figure. 2 shows the calculated proton and neutron pairing gaps $\tilde{\Delta}$ versus the rotational frequency $\hbar\omega$ for the alternating-parity bands in even-even nuclei ^{236,238}U and ^{238,240}Pu, and the parity-doublet bands in odd-A nuclei ^{237}U and ^{239}Pu. The effective pairing strengths are the same for the PNC-CSM calculations for the reflection-asymmetric nuclei and reflection-symmetric nuclei. As shown in Fig. 2, the pairing gaps $\tilde{\Delta}$ in the reflection-asymmetric nuclei are almost larger than those in the reflection-symmetric nuclei for both protons and neutrons. The pairing gaps decrease with increasing rotation frequency $\hbar\omega$, and significantly decrease for the neutrons in the odd-A nuclei ^{237}U and ^{239}Pu.

In order to investigate the effect of the rotational frequency on the pairing gap, we study the relative pairing reduction on the rotational frequency $\hbar\omega = 0.30$ MeV compared with the bandhead $\hbar\omega = 0.00$ MeV in the reflection-

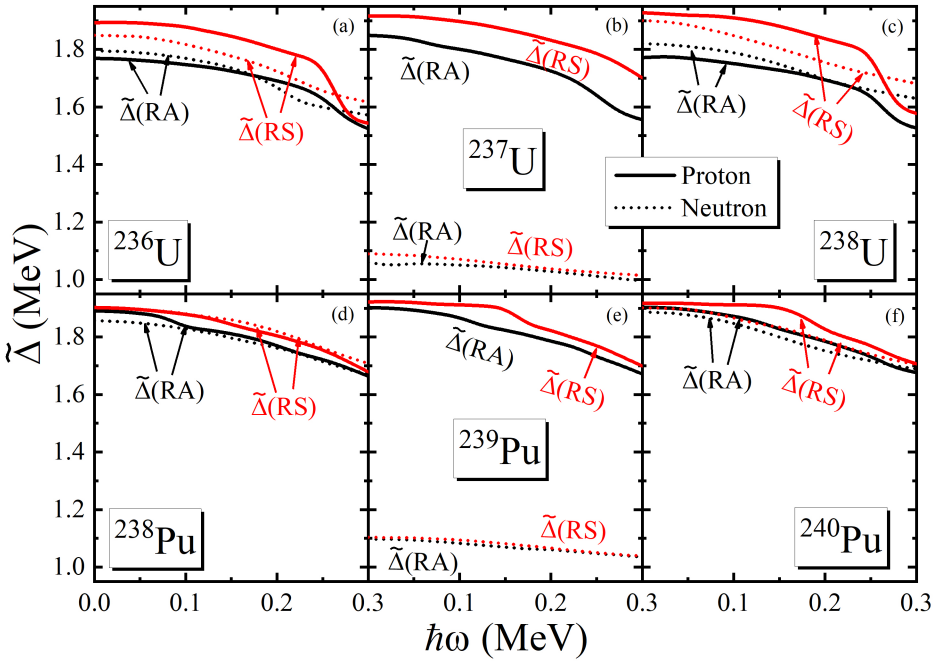

Fig. 2 (Color online) The calculated proton and neutron pairing gaps $\tilde{\Delta}$ versus the rotational frequency $\hbar\omega$ for the alternating-parity bands in even-even nuclei ^{236,238}U and ^{238,240}Pu, and parity-double bands in odd-A nuclei ^{237}U and ^{239}Pu. The PNC-CSM calculations in the reflection-asymmetric nuclei are denoted by black lines, and those in the reflection-symmetric nuclei (without ε_3 deformation) are denoted by red lines. The solid and dotted lines are for protons and neutrons, respectively.

asymmetric nuclei ^{236}U, the calculated results are:

$$\frac{\delta\tilde{\Delta}_p}{\tilde{\Delta}_p} = \frac{\tilde{\Delta}_p(^{236}\mathrm{U}, \hbar\omega = 0.30\mathrm{MeV}) - \tilde{\Delta}_p(^{236}\mathrm{U}, \omega = 0)}{\tilde{\Delta}_p(^{236}\mathrm{U}, \omega = 0)} = 13.8\%,$$
$$\frac{\delta\tilde{\Delta}_n}{\tilde{\Delta}_n} = \frac{\tilde{\Delta}_n(^{236}\mathrm{U}, \hbar\omega = 0.30\mathrm{MeV}) - \tilde{\Delta}_n(^{236}\mathrm{U}, \omega = 0)}{\tilde{\Delta}_n(^{236}\mathrm{U}, \omega = 0)} = 12.5\%.$$

The results are very similar for other nuclei, which are not shown here. For both protons and neutrons, it can be seen that the pairing gaps decrease by about 10% at the frequency $\hbar\omega = 0.30$ MeV compared with those at the bandhead $\hbar\omega = 0.00$ MeV. These result in the gradual increase of $\mathcal{J}^{(1)}$ versus rotational frequency in all nuclei.

Comparing Fig. 2(a), 2(d) and Fig. 2(b), 2(e), it is seen that the pairing gaps of neutron significantly decrease in the odd-A nuclei ^{237}U and ^{239}Pu. To see the effect of Pauli block effects on the pairing gap, we study the neutron pairing gaps of these nuclei at the bandhead $\hbar\omega = 0.00$ MeV, the calculated results are:

$$\frac{\delta\tilde{\Delta}_n}{\tilde{\Delta}_n} = \frac{\tilde{\Delta}_n(^{237}\mathrm{U}, \mathrm{RA}) - \tilde{\Delta}_n(^{236}\mathrm{U}, \mathrm{RA})}{\tilde{\Delta}_n(^{236}\mathrm{U}, \mathrm{RA})} = 41.0\%,$$
$$\frac{\delta\tilde{\Delta}_n}{\tilde{\Delta}_n} = \frac{\tilde{\Delta}_n(^{239}\mathrm{Pu}, \mathrm{RA}) - \tilde{\Delta}_n(^{238}\mathrm{Pu}, \mathrm{RA})}{\tilde{\Delta}_n(^{238}\mathrm{Pu}, \mathrm{RA})} = 40.9\%.$$

We can see that the pairing gaps decrease about 40% in the odd-A nuclei compared with the neighboring even-even nuclei, which lead to the significant increase of $\mathcal{J}^{(1)}$ in the $s = -i$ bands in the odd-A nuclei [see Figs.1(a), 1(c), 1(e) and 1(g)].

To see the effect of the octupole deformation on the pairing gap, we study the pairing gaps at the bandhead $\hbar\omega = 0.00$ MeV in the ^{236}U and ^{238}Pu with reflection-asymmetric deformation and reflection-symmetric deformation, the calculated results for ^{236}U are:

$$\frac{\delta\tilde{\Delta}_p}{\tilde{\Delta}_p} = \frac{\tilde{\Delta}_p(^{236}\mathrm{U}, \mathrm{RA}) - \tilde{\Delta}_p(^{236}\mathrm{U}, \mathrm{RS})}{\tilde{\Delta}_p(^{236}\mathrm{U}, \mathrm{RS})} = 6.6\%,$$
$$\frac{\delta\tilde{\Delta}_n}{\tilde{\Delta}_n} = \frac{\tilde{\Delta}_n(^{236}\mathrm{U}, \mathrm{RA}) - \tilde{\Delta}_n(^{236}\mathrm{U}, \mathrm{RS})}{\tilde{\Delta}_n(^{236}\mathrm{U}, \mathrm{RS})} = 2.9\%,$$

and the calculated results for ^{238}Pu are:

$$\frac{\delta\tilde{\Delta}_p}{\tilde{\Delta}_p} = \frac{\tilde{\Delta}_p(^{238}\mathrm{Pu}, \mathrm{RA}) - \tilde{\Delta}_p(^{238}\mathrm{Pu}, \mathrm{RS})}{\tilde{\Delta}_p(^{238}\mathrm{Pu}, \mathrm{RS})} = 0.6\%,$$
$$\frac{\delta\tilde{\Delta}_n}{\tilde{\Delta}_n} = \frac{\tilde{\Delta}_n(^{238}\mathrm{Pu}, \mathrm{RA}) - \tilde{\Delta}_n(^{238}\mathrm{Pu}, \mathrm{RS})}{\tilde{\Delta}_n(^{238}\mathrm{Pu}, \mathrm{RS})} = 2.4\%.$$

We can see that the pairing gap decrease in the reflection-asymmetric nuclei in the PNC-CSM calculation. Furthermore, the pairing gap decrease more larger when the octupole deformation increasing [see Figs. 2(a) and 2(d)]. Therefore,

the octupole correlations give a certain effect on the increase of $J^{(1)}$ in the reflection-asymmetric nuclei. The results are very similar for other nuclei, which are not shown here.

4 Summary

The reflection-asymmetric nuclei ^{236,237,238}U and ^{238,239,240}Pu were investigated by the cranked shell model with pairing correlations treated by the particle-number-conserving method. The experimental moments of inertia of the alternating-parity bands in the even-even nuclei ^{236,238}U and ^{238,240}Pu and the parity-doublet bands in the odd-A nuclei ^{237}U and ^{239}Pu are well reproduced by the PNC-CSM calculations. There are significant effects of rotation, Pauli blocking effects and octupole deformation on the pairing gaps in these nuclei. A detailed investigation of the pairing shows that the increase of moments of inter $J^{(1)}$ can be attributed to the effects of pairing reduction due to rotation, Pauli blocking effects and octupole deformation in the reflection-asymmetric U and Pu isotopes.

References

[1] AHMAD I, BUTLER P A. Annu Rev Nucl Part Sci, 1993, 43(1): 71. https://doi.org/10.1146/annurev.ns.43.120193.000443.

[2] LEVON A I, DE BOER J, LOEWE M, et al. Eur Phys J A, 1998, 2 (1): 9.

[3] LIANG C F, PARIS P, SHELINE R K, et al. Phys Rev C, 1998, 57: 1145. https://link.aps.org/doi/10.1103/PhysRevC.57.1145.

[4] ZAMFIR N V, KUSNEZOV D. Phys Rev C, 2003, 67: 014305. https://link.aps.org/doi/10.1103/PhysRevC.67.014305.

[5] BUCK B, MERCHANT A C, PEREZ S M. J Phys G: Nucl Part Phys, 2008, 35(8): 085101. https://dx.doi.org/10.1088/0954-3899/35/8/085101.

[6] PARR E, SMITH J F, GREENLEES P T, et al. Phys Rev C, 2022, 105: 034303. https://link.aps.org/doi/10.1103/PhysRevC.105.034303.

[7] WARD D, ANDREWS H, BALL G, et al. Nucl Phys A, 1996, 600(1): 88. https://www.sciencedirect.com/science/article/pii/0375947495004904. DOI: https://doi.org/10.1016/0375-9474(95)00490-4.

[8] WIEDENHÖVER I, JANSSENS R V F, HACKMAN G, et al. Phys Rev Lett, 1999, 83: 2143. https://link.aps.org/doi/10.1103/PhysRevLett.83.2143.

[9] WANG X, JANSSENS R V F, CARPENTER M P, et al. Phys Rev Lett, 2009, 102: 122501. https://link.aps.org/doi/10.1103/PhysRevLett.102.122501.

[10] ZHU S, CARPENTER M P, JANSSENS R V F, et al. Phys Rev C, 2010, 81: 041306. https://link.aps.org/doi/10.1103/PhysRevC.81.041306.

[11] SPIEKER M, BUCURESCU D, ENDRES J, et al. Phys Rev C, 2013, 88: 041303. https://link.aps.org/doi/10.1103/PhysRevC.88.041303.

[12] ROBLEDO L M, BERTSCH G F. Phys Rev C, 2011, 84: 054302. https://link.aps.org/doi/10.1103/PhysRevC.84.054302.

[13] CHEN X C, ZHAO J, XU C, et al. Phys Rev C, 2016, 94: 021301. https://link.aps.org/doi/10.1103/PhysRevC.94.021301.

[14] DOBROWOLSKI A, MAZUREK K, GÓzźD zź A. Phys Rev C, 2018, 97: 024321. https://link.aps.org/doi/10.1103/PhysRevC.97.024321.

[15] CHEN Y S, GAO Z C. Phys Rev C, 2000, 63: 014314. https://link.aps.org/doi/10.1103/PhysRevC.63.014314.

[16] HE X T, LI Y C. Phys Rev C, 2020, 102: 064328. DOI: 10.1103/PhysRevC.102.064328.

[17] ZENG J Y, CHENG T S. Nucl Phys A, 1983, 405(1): 1.

[18] LIU S, ZENG J, ZHAO E, et al. Phys Rev C, 2002, 66: 024320.

[19] ZHANG Z H. Nucl Phys A, 2016, 949: 22.

[20] HE X T, LI Y C. Phys Rev C, 2018, 98(6): 064314. DOI: 10.1103/PhysRevC.98.064314.

[21] ZHANG J, HE X T, LI Y C, et al. Phys Rev C, 2023, 107: 024305. https://link.aps.org/doi/10.1103/PhysRevC.107.024305.

[22] NAZAREWICZ W, OLANDERS P. Nucl Phys A, 1985, 441(3): 420. https://www.sciencedirect.com/science/article/pii/037594748590154X. DOI: https://doi.org/10.1016/0375-9474(85)90154-X.

[23] ZHANG Z H, HE X T, ZENG J Y, et al. Phys Rev C, 2012, 85: 014324. DOI: 10.1103/PhysRevC.85.014324.

[24] NILSSON S G, TSANG C F, SOBICZEWSKI A, et al. Nucl Phys A, 1969, 131(1): 1. https://www.sciencedirect.com/science/article/pii/0375947469908094. DOI: https://doi.org/10.1016/0375-9474(69)90809-4.

[25] WU X, ZHANG Z H, ZENG J Y, et al. Phys Rev C, 2011, 83: 034323. https://link.aps.org/doi/10.1103/PhysRevC.83.034323.

转动、堵塞效应和八极形变对 U 和 Pu 同位素对关联的影响

章 骏[1]，贺晓涛[2]

（1. 南京航空航天大学物理学院, 南京 210016;
2. 南京航空航天大学材料科学与技术学院, 南京 210016）

摘要：通过在 Nilsson 势中引入八极关联相互作用，基于推转壳模型（CSM）下的粒子数守恒方法（PNC）处理包含单极和四极对力的哈密顿量，研究了反射不对称（RA）原子核的基态转动带。基于此，PNC-CSM 的计算结果重现了轻锕系区偶偶核 ^{236,238}U 和 ^{238,240}Pu 的交替宇称带，以及奇-A 核 ^{237}U 和 ^{239}Pu 的宇称带双重带的转动惯量实验值。与相邻偶偶核 ^{236,238}U 和 ^{238,240}Pu 相比，奇-A 核 ^{237}U 和 ^{239}Pu 的 $s=-i$ 内禀转动带的转动惯量增加了 50% ∼ 60%。这些增加的转动惯量主要是由费米面附近中子轨道的泡利堵塞效应减弱了中子体系的对关联导致。U 和 Pu 同位素中，转动惯量随着转动频率缓慢增加则可以解释为转动使得体系的对关联减弱。在低频率区，反射不对称原子核的转动惯量明显高于相对应的反射对称（RS）原子核的转动惯量。并且，与反射对称原子核相比，较大的八极形变将导致反射不对称原子核体系的对关联减弱更加明显。

关键词：八极关联; 推转壳模型; 粒子数守恒方法; 交替宇称带; 宇称双重带; 对关联

收稿日期：2024-03-18；　**修改日期：**2024-03-18
基金项目：国家自然科学基金资助项目 (U2032138, 11775112)
通信作者：贺晓涛，E-mail: hext@nuaa.edu.cn